

Effect of Channel Aspect Ratio and Inclination Angle on Flow and Mixing Performance of a Microdevice—A CFD Study

Urooj Fatima^a, M. Shakaib^b, *, **, and Inayatullah Memon^a

^a Department of Chemical Engineering, NED University of Engineering and Technology, Karachi, Pakistan

^b Department of Mechanical Engineering, NED University of Engineering and Technology, Karachi, Pakistan

*e-mail: mshakaib@neduet.edu.pk

**e-mail: mshakaib@live.com

Received March 7, 2020; revised September 30, 2020; accepted November 20, 2020

Abstract—This work includes a 3D computational fluid dynamics study on rectangular-shaped micromixers. Initially, T-shaped micromixer types are considered with various width/height ratios for the inlet and the outlet channels and the results are presented in terms of velocity profiles, mass fraction distribution, pressure drop, mixing efficiency and mixing effectiveness. The findings show that the mixers with an outlet channel aspect ratio (width to height ratio) of 2–2.5 yields better mixing performance. The flow separation at the entrance of the mixing channel leads to formation of recirculation zones which promotes mixing. The effect of confluence angle is also examined for a few aspect ratios. The comparison of mixing parameters indicates that large confluence angles are suitable for the micromixing devices.

Keywords: computational fluid dynamics, micromixer, confluence angle, mixing efficiency, pressure drop

DOI: 10.1134/S0040579521030052

INTRODUCTION

Microfluidic devices have been extensively studied upon over the past few years because of the promising and diverse applications it offers in chemical and biological systems, biomedical devices, environmental monitoring and non-destructive analytical techniques. Among the various microdevices, micromixer is a device/component used for many processes such as crystallization, polymerization, dispersion, emulsification and DNA purification [1–6]. Mixing greatly affects vital processing parameters, for example, product yield, selectivity, analysis time as well as cost effectiveness, safety and reaction controllability. The characterization and evaluation of mixing performance, therefore, is of much significance [7–9].

A micromixer includes flow of at least two fluids which enter through their respective inlets and then mix in a common channel. Based on the driving force for mixing, the micromixers can be of an active or a passive type. The advantages of passive type mixers are that their fabrication is relatively simple and they do not require any external means for moving or agitating the fluids [6, 10, 11]. In passive mixers, laminar flow conditions usually prevail and the molecular diffusion, in addition to the mass convection, is an important mechanism that governs mixing. A limitation of this type is that the rate of mass transport is low and a sufficient channel length or residence time is required for mixing. A method that can be adopted to increase the

rate of mixing is to modify the geometry of the micromixer device and generate secondary flow components.

Due to the importance of the passive mixer device, many studies have examined the techniques that can improve mixing performance through the enhancement of secondary flow motions. For example, Rahimi et al. [12] compared various mixer shapes such as T, Y, and oriented Y-spatial. The experiments at various Reynolds number revealed that suitable spatial shapes of channels can result in considerable improvement in micromixing. Hsieh et al. [13] experimentally studied characteristics of Y-type mixers at different electric field strengths. A major effect was found of Joule heating on micromixer performance. The CFD work of Lobasov et al. [14] examined the effect of channel width and height on mixing efficiency and pressure drop of T-shaped channels. The experimental and numerical investigations by Wong et al. [15] reported that the vortices generated at the junction enhance mixing. Silva et al. [16] showed superior mixing quality through a T-shaped micromixer under asymmetric flow conditions. Ansari et al. [17] carried out experimental study and suggested that simple geometrical variations result in vortex flow that enables the fluid streams to intertwine with each other and result in high mixing quality. The experimental work of Calado et al. [18] suggested five different mixing and flow regimes for micromixing devices. A study by

Table 1. T-shaped micromixers considered in this study

Micromixer name (type) and dimensions		MM-01	MM-02	MM-03	MM-04	MM-05	MM-06
Inlet channels	$h, \mu\text{m}$	200	200	200	200	160	125
	$w, \mu\text{m}$	200	200	200	200	250	320
Outlet channel	$H, \mu\text{m}$	200	200	200	200	160	125
	$W, \mu\text{m}$	200	300	400	500	500	640

You et al. [19] demonstrated that by varying the confluence angle, interaction of vortices and mixing process can be facilitated. Chen et al. [20] performed experiments and finite element simulations for tree-shaped micromixers. The mixing performance was found to be increasing with the increase in fractal level. Soleymani et al. [21] compared different types of micromixer configurations. At higher flow rate, TT-mixer was found to be more suitable than the ordinary T-mixer. A numerical work of Cortes-Quiroz et al. [22] included comparison of a 3D T-mixer and an ordinary T-mixer. The 3D mixer resulted in higher mixing indices. Recently, the present authors [23] tested the effect of flow rate ratio and confluence angle in asymmetric mixers with circular microchannels. In addition to relatively less complicated modifications of microchannels, several studies proposed complex methods to achieve high mixing efficiency such as inclusion of obstacles in the mixing channel [24, 25], varying the internal structure of mixing channel [26–31] and changing the shape of the microchannels [32, 33].

The review of the literature demonstrates that numerous studies have been conducted in the recent past for evaluating the commonly used mixer designs and proposing improvements so that better mixing performances can be obtained. From the previous papers, it is recognized that the geometric parameters can have an impact on the mixing performance in microfluidic devices. To the authors' knowledge, however, no study exists in which the effect of channel aspect ratio is examined at different inclination/confluence angles. In the present work, it is shown that simple geometric adjustments such as aspect ratios of the rectangular shaped inlet and outlet channels can have considerable effect on mixing. Suitable channels height/widths and channel inclination angles which exhibit superior mixing performance at two different Reynolds number are also identified.

MODELING PROCEDURE

CFD simulations are carried out firstly for predicting mixing characteristics of a T-shaped ($\theta = 90^\circ$) microchannel device. In comparison to the earlier studies, the effect of aspect ratios of both inlet and outlet channels (w/h and W/H) are examined. The aspect ratios which result in better mixing quality/efficiency are simulated at different confluence angles.

Table 1 shows the considered micromixer dimensions. For all the cases, the inlet cross sectional area is same. The height of inlet channels equals the height of outlet channel (i.e. $h = H$). In MM-01 to MM-04, the w/h ratio is 1; in MM-05 and MM-06, this ratio is about 1.5 and 2.5, respectively. The W/w ratio varies from 1–2.5.

The schematic diagram of the geometry constructed for the 3D investigations is shown in Fig. 1. It consists of two inlet channels and a mixing/outlet channel. A tracer solution flows in one inlet channel while water flows in the other. The inlet and the outlet channel lengths of the actual microdevices depend on the type of application. To reduce the size of the computational domain, the inlet channel lengths (L_t and L_w) are 500 μm for all the cases. Since mixing of fluids continues up to a sufficiently large distance, the mixing channel length is relatively more and set to 3000 μm . The angle of confluence θ that is the angle between the vertical direction (y -axis) and any of the inlet channels is varied for a few aspect ratios.

A structured mesh is used for the computational region. In the mixing zone/junction and adjacent to the walls, the mesh density is higher. The mesh cells sizes gradually increase away from the junction. The optimal number of cells is obtained by continuous refinement of the mesh so that the numerical diffusion is reduced. The plot of mixing efficiency at several grids in Figure 2 shows that the efficiency varies when grid contains less number of cells. The difference in mixing efficiency values reduce and is less than 1% when cells are increased from 8.7×10^5 to 1.61×10^6 . Similarly, the mass fraction distribution is same at these two different grids as shown in Fig. 2b. A grid containing about 8.7×10^5 control volumes, thus, is considered to be suitable for minimizing the numerical errors and providing grid-independent solutions.

The tracer fluid is assumed to have same physical properties as that of water. The value of density ρ is 998 kg/m^3 and viscosity μ is 0.001 kg/m s . The diffusivity D_{BA} of tracer solution in water is taken as $1.5 \times 10^{-9} \text{ m}^2/\text{s}$ [34]. The microdevice is assumed to be horizontally placed so that the gravitational effect is ignored. Velocity inlet and pressure outlet are the boundary conditions for inlets and outlet, respectively. Continuity, momentum and concentration equations are the governing equations solved using CFD code ANSYS Fluent. Laminar steady flow and species transport without reaction models are used. Second

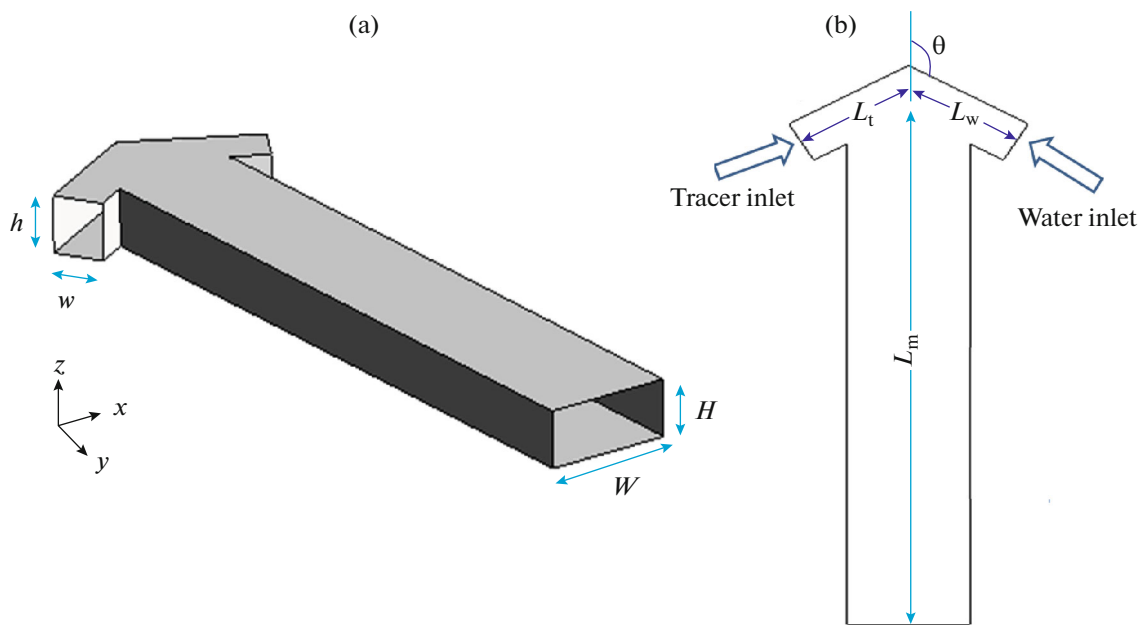


Fig. 1. Computational domain for micromixers: (a) 3D view and (b) top view.

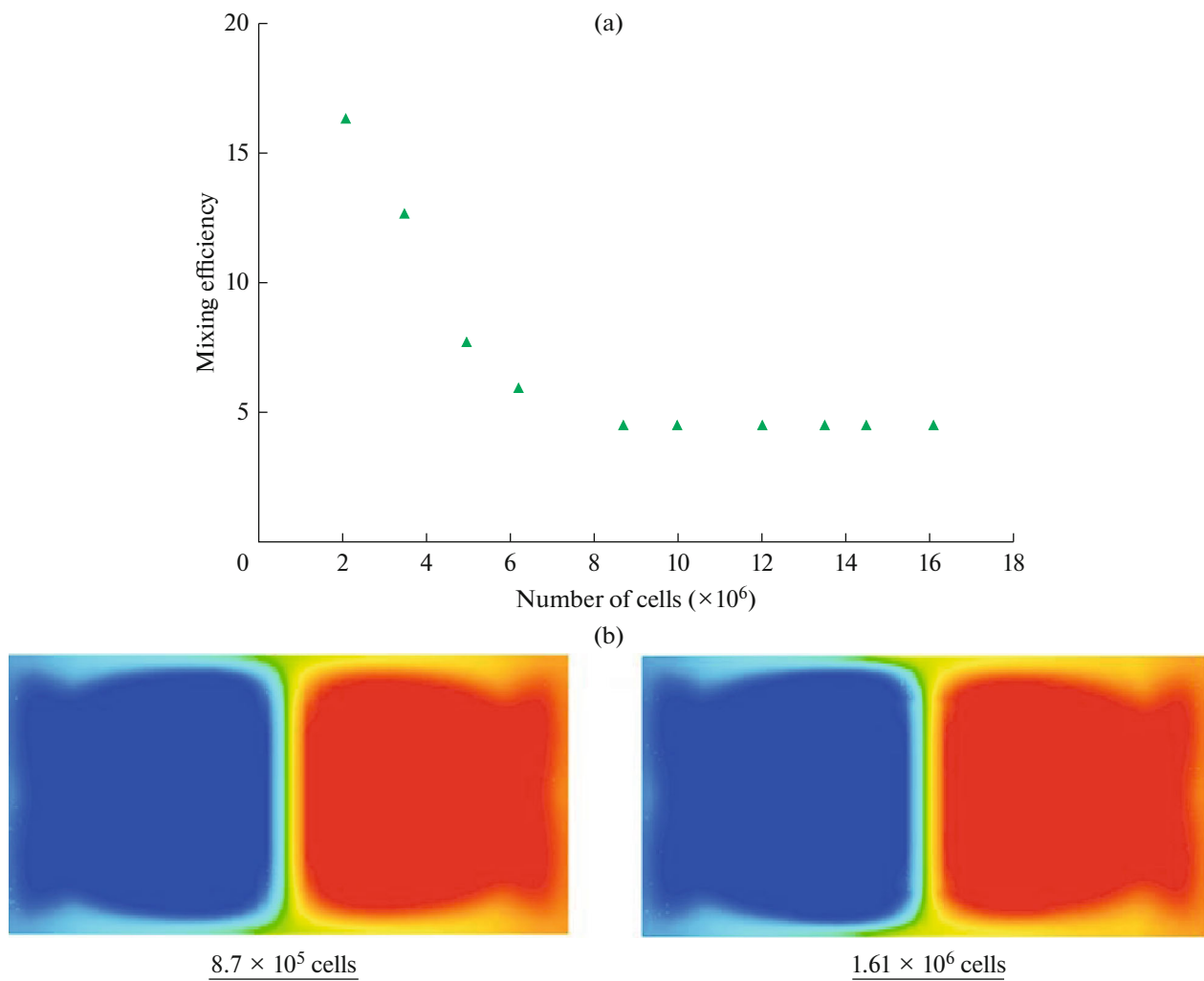


Fig. 2. (a) Mixing efficiency versus number of cells and (b) mass fraction contours at $x = 1000 \mu\text{m}$ (MM-03).

order upwind scheme is used for discretization of the momentum and the concentration/mass transfer equations. SIMPLE (Semi-Implicit Method for Pressure Linked Equations) algorithm is used to couple pressure and velocity fields. The convergence criterion for the residuals of the continuity, the momentum and the mass fraction is set as 10^{-5} . Two different Reynolds numbers $Re = 120$ and 180 are chosen to investigate the mixing performance. The Reynolds number is defined as:

$$Re = \frac{u_{av} d_h}{\nu}, \quad (1)$$

where u_{av} is the average velocity in the mixing (outlet) channel, d_h is the hydraulic diameter and ν is the kinematic viscosity. The hydraulic diameter is determined as:

$$d_h = \frac{2HW}{(H+W)}. \quad (2)$$

In order to quantify mixing performance of a microchannel device, the common relations used are based on standard deviation or variance of species mass fraction. In this paper, mixing efficiency (η) is calculated which is also based on the standard deviation of the local mass fractions. The η relation is the same as used in the various other studies [7, 8, 14] and is given in equation (3)

$$\eta = 1 - \frac{\sigma}{\sigma_0}, \quad (3)$$

Where σ_0 is the maximum standard deviation of tracer mass fraction and σ is the standard deviation of mass fraction at the outlet section in any mixer. The standard deviation σ can be predicted through weighted relations such as by including cell face area, volume, velocity as weighting parameters or unweighted relation by simply considering the mass fraction values at different cells. The standard deviation in this work is obtained using velocity weighted formula [35, 36]. The mathematical relation is:

$$\sigma^2 = \frac{1}{Q_t} \int u_y (c - \bar{c})^2 dA. \quad (4)$$

In equation (4), Q_t is total volumetric flow rate in mixing channel

A device geometry which results in enhanced mixing often requires more pressure or energy for the fluid flow. Thus, for indicating the optimal geometries, in addition to mixing efficiency, a performance indicator termed as 'mixing effectiveness' (ME) is calculated. The ME relation as proposed by Kockmann et al. [7] is as follows:

$$ME = \frac{d_h}{u_{av} t_m} Eu, \quad (5)$$

where Euler number Eu is $\Delta p / \rho u_{av}^2$ and t_m is mixing time.

Low Euler numbers and mixing times and thus high mixing effectivenesses are desirable. The devices are considered superior when both and ME have high values.

The length of mixing channel should be sufficiently large for determining the mixing time. As the diffusion coefficient considered in this paper is low and the outlet channel length is less due to computational limitations, t_m cannot be calculated directly. The mixing time, therefore, is estimated using residence time t_r and efficiency η as given in equation (6):

$$t_m = \frac{t_r}{\eta}. \quad (6)$$

The momentum and mass transport processes are related and the increase or decrease of mixing rate can be explained in terms of circulation ω_y . Circulation predicts flow rotational movements and is calculated using equation (7).

$$\omega_y = \int \left(\frac{\partial V_z}{\partial x} - \frac{\partial V_x}{\partial z} \right) dx dz. \quad (7)$$

The present numerical results are compared with the work of Aoki et al. [8] in terms of pressure drop. The comparison is reported in terms of friction factor f , which is a dimensionless form of pressure drop. f is calculated using equation (8)

$$f = \frac{\Delta P d}{L} \frac{2}{\rho u_{av}^2}. \quad (8)$$

RESULTS AND DISCUSSION

The flow behavior in various micromixers is explained with the help of velocity profiles in Fig. 3. The velocity plots versus x at a y -location of 0.5 mm (measured from the inlet section of the mixing channel) show that the local velocity increases near the central region and decreases to zero at the walls as expected. It is noticed that in the geometry with small outlet channel width or W/H ratio (MM-01), the velocity profile is almost parabolic. As the aspect ratio (W/H) increases (MM-02 – MM-04), the profile changes and more variation in the slope of the velocity curve is observed. This is due to an increase in the size of the separation (low velocity) zone near the walls when the fluids turn into the mixing channel. The velocity plots of MM-02–MM-04, thus show a point of inflexion which is attributed to significant flow separation and rotation. The comparison of MM-04 and MM-05 indicates that when width W is same but height H is reduced, the velocity profile again has a parabolic shape (without point of inflexion). This means that a decrease in channel height reduces the flow separation effect. When aspect ratio W/H is further increased (MM-06), a continuous variation in the velocity curve slope is again observed.

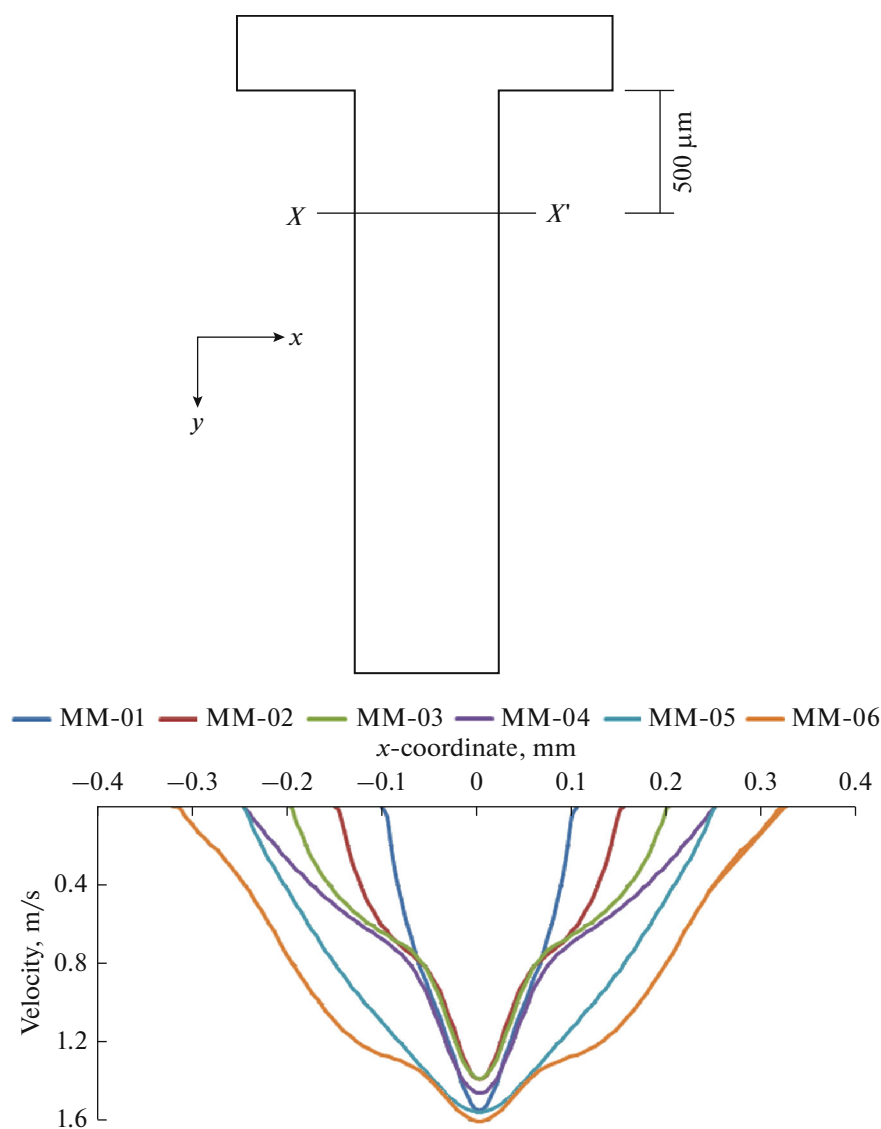


Fig. 3. Velocity profiles on transversal lines at 500 μm of the mixing channel ($\text{Re} = 180$).

Velocity vectors in the six considered microchannel geometries at a distance $y = 500 \mu\text{m}$ are depicted in Fig. 4. The flow behavior for MM-01 to MM-04 shows that as the width increases, the sizes of the vortices increase. The increase in the size of the vortices or recirculation regions is anticipated to facilitate the interfacial contact and mixing of the two fluids. In mixers MM-05 and MM-06, the strength of vortices tends to diminish due to decreased height.

From the literature, it is known that three basic flow regimes namely the stratified, vortex and engulfment regimes exist within the laminar range. At very low Reynolds numbers, stratified regime exists in which the two fluids follow a separate and well-defined path without any noticeable rotational motion. With the increase of Reynolds number, vortex regime begins in which flow is symmetric but recircu-

lation regions are formed at the entrance of the mixing channel. In the engulfment range, the fluids cross the geometrical plane of symmetry (yz plane in this paper) of the mixer. The streamlines of the two fluids in this case appear to interlace. The critical value at which the engulfment starts generally is when $\text{Re} \geq 150$ depending upon the aspect ratio [7, 21]. The velocity line plots and vectors in Figs. 3 and 4, although show significant vortices formation but the flow patterns seem to be symmetric. A possible reason is that $\text{Re} = 180$ (a maximum value considered in this paper) lies in the beginning of the engulfment flow regime. A relatively higher of Reynolds number such as $\text{Re} \geq 200$ might lead to an asymmetric flow behavior as observed in previous studies [19, 21, 37].

The circulation values calculated using equation (7) at the xz cross-sectional plane are also shown

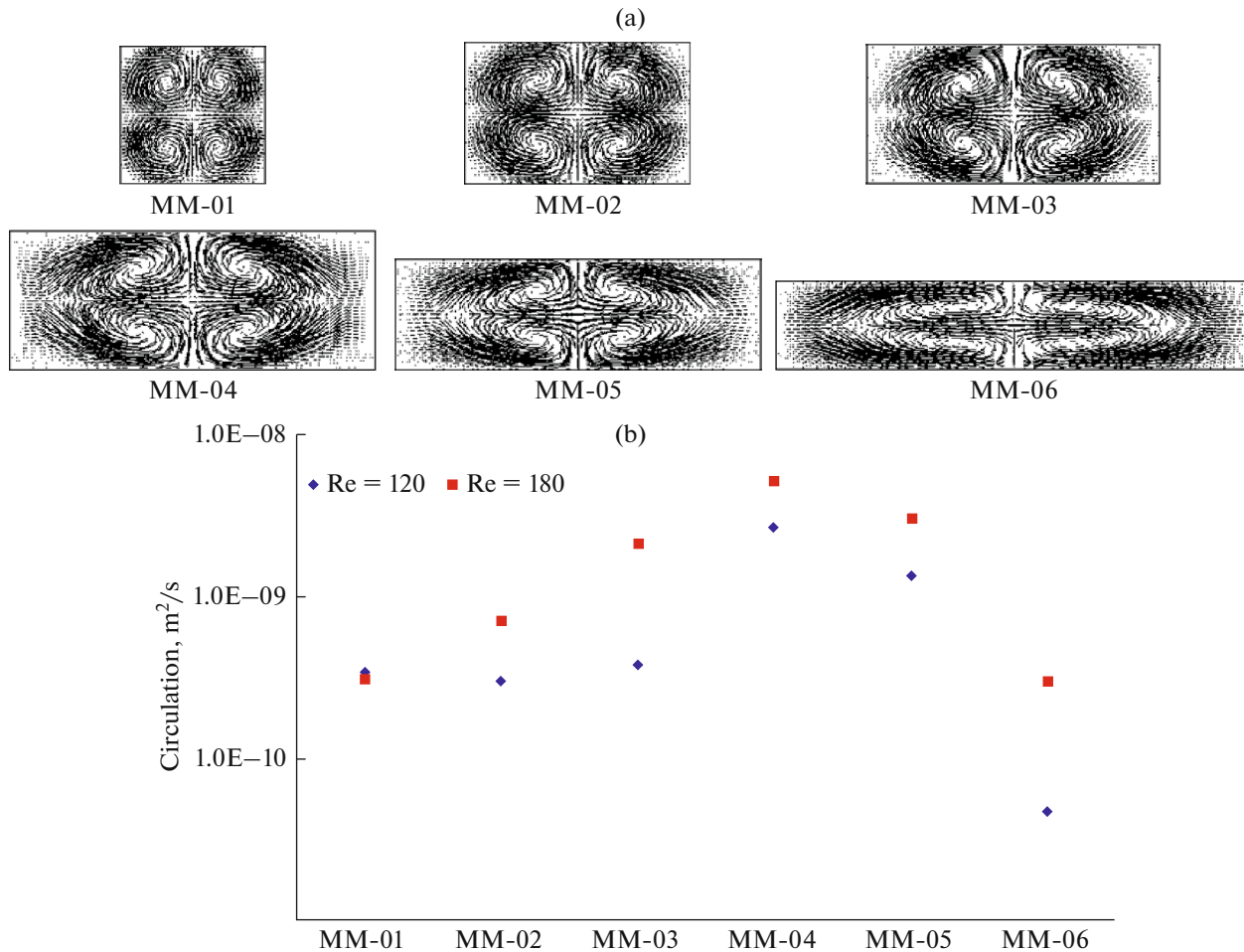


Fig. 4. (a) Velocity vectors and (b) circulation for different micromixer types at a plane 500 μm .

(Fig. 4b). A higher Reynolds number usually results in a higher value of circulation. The circulation increases as the width of the channel increases (when height is constant) as seen for MM-01–MM-04 while it decreases considerably in MM-05 and MM-06 which have reduced heights. The circulation results are consistent with the information inferred from vectors plots (Fig. 4a) in which less rotational flow motion is seen at small heights.

The mass fraction contours in micromixers in Fig. 5 indicate that within the mixers of same channel height (MM-01–MM-04), the region for species diffusion is limited at the fluids interface i.e. central vertical portion when channel width W is small. When width is increased, in addition to mixing at the interface of the two fluids, the mixing or variation of local mass fractions is also found in the top and the bottom portions of the outlet channel. In the cases of MM-03 or MM-04, the local mass fraction varies from 0.3–0.7 in the central plane as well as in the top and bottom locations. This shows that the convective effects become significant when width is relatively large. The decrease in channel height in geometries MM-05 and

MM-06 hinders the convection mode and confines the mixing region only at the fluids interface. The difference in mixing rates can also be linked to the type of flow regime i.e. vortex or engulfment. In MM-01 and MM-02, the width of outlet channel is small, whereas in MM-05 or MM-06 the channel height is reduced. The flow in these types is expected to be in the vortex regime. On the other hand, due to increased width or hydraulic diameter of the outlet channel in MM-03 or MM-04, the regime is possibly changed from vortex to engulfment.

The comparison in terms of pressure drop and mixing parameters is shown in Figure 6. The increase in width at constant height decreases pressure drops as can be seen for mixers MM-01–MM-04. The decrease in height increases pressure drop such as in MM-05 and MM-06 due to increased viscous drag. The mixing efficiency η is found relatively high for micromixers MM-03 and MM-04 and significantly low for MM-05 and MM-06. The results of pressure drop and mixing efficiency of various mixers can be considered important findings of the paper as it can be suggested that the mixers with appropriate aspect

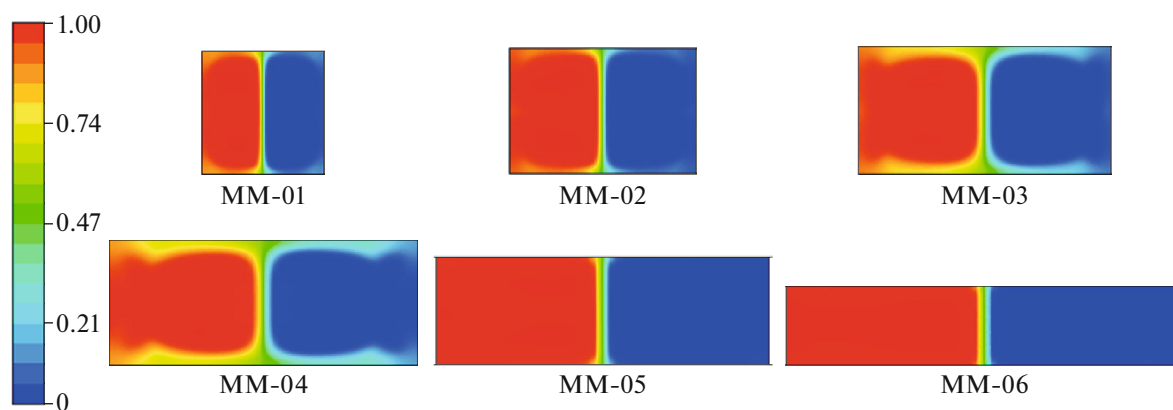


Fig. 5. Mass fraction contours at outlet of a mixing channel in a T-shaped device with different aspect ratios.

ratios can considerably increase the mixing performance. Further, the increase of aspect ratio is advantageous up to a certain value. The reduction in height to increase aspect ratios stabilizes the flow which decreases mixing efficiency η . The drop in η is directly related to the velocity distribution and the circulation obtained in Fig. 4. The high mixing efficiencies in MM-03 or MM-04 are due to significant flow circulation that decrease local velocities at certain locations and provide more residence time for the species to mix. The mixers with small height (e.g. MM-06), on the other hand, have more axial flow which reduces vorticity or circulation and hence the mixing rate. The comparison of mixing effectiveness indicates that for the mixers with same channel height, increase in outlet width increases the effectiveness about 2–3 times. The reason is that the geometries with large widths result in reduced frictional loss and provide more freedom for fluids to mix. The decrease in the height of the microchannel, for example in the cases of MM-05 or MM-06, however, significantly increases viscous losses and decreases interaction of the two fluids.

Based on the results of mixing effectiveness (ME), MM-03 and MM-04 are selected to investigate the effect of the inclination of inlet channel (or confluence angle) on mixing performance. The effect of confluence angles on flow pattern is shown in Fig. 7. The general flow features, similar to the standard T-shaped geometry, are, a high velocity region in the center of the mixing channel and a low velocity region at the corners due to separation of flow. When angle is small, the high velocity zone is thicker whereas the size of low velocity region is less. The increase in angle θ not only increases the size of low velocity recirculation region at the corner/inlet of mixing channel section but also creates an additional low velocity region at the junction of the two inlet channels. The fluid behavior in xz (transverse) plane given in Fig. 8 shows that when angles are small such as $\theta = 45^\circ$ or 60° , the flow direction is mostly axial as it appears from the size of velocity vector. The increase in angle θ increases flow

motion in the non-axial direction. The flow movements in transverse direction are found more obvious when θ is 90° – 135° .

The mass fraction contours in Fig. 9 reveal that at small confluence angles, the two fluids pass through the outlet channel as isolated streams without any appreciable mixing. The mixed fluid layers exist only at the contact surface of the two fluids. When the angle is increased, the two fluids intertwine at the junction of the inlet channels before they enter into the outlet channel. This develops a low-velocity flow circulation region (as was seen in Fig. 7) which augments mixing. The mixed zone, that is the zone which has average values of concentrations, thus, is found to be thick in the devices with large angles (e.g. $\theta = 120^\circ$). The contours of mass fraction of tracer versus y distance are shown in Fig. 10. The variation in mass fraction distribution is mostly up to about $1000 \mu\text{m}$. After this length, the mixing is less significant. The comparison of the three angles shows that in the case of angle 60° , the mixed fluids layer (with concentration/mass fraction close to 0.5) initially is thin at the interface. As the fluid moves ahead, the thickness of this layer increases. The mixing effect also starts appearing near the top and bottom surfaces when $y = 500 \mu\text{m}$. In the 90° geometry, the mixed fluids layer is relatively thick in the center, particularly, when $y \leq 700 \mu\text{m}$. The mixed fluids layer i.e. the region of average concentration then shifts from center to the side walls as can clearly be noticed when $y = 1000 \mu\text{m}$. In the 120° micromixer, when $y < 500 \mu\text{m}$, the mixed fluids region is relatively thick at the top and the bottom walls. At 700 and $1000 \mu\text{m}$, spots or small regions of low concentration in tracer fluid and spots of relatively high tracer concentration in water are also seen. This indicates a disturbed flow pattern which is probably due to the presence of engulfment flow regime in the mixer with $\theta = 120^\circ$.

The pressure drop, mixing efficiency η and effectiveness (ME) are determined for various confluence angles and are shown in Fig. 11. In the cases of small

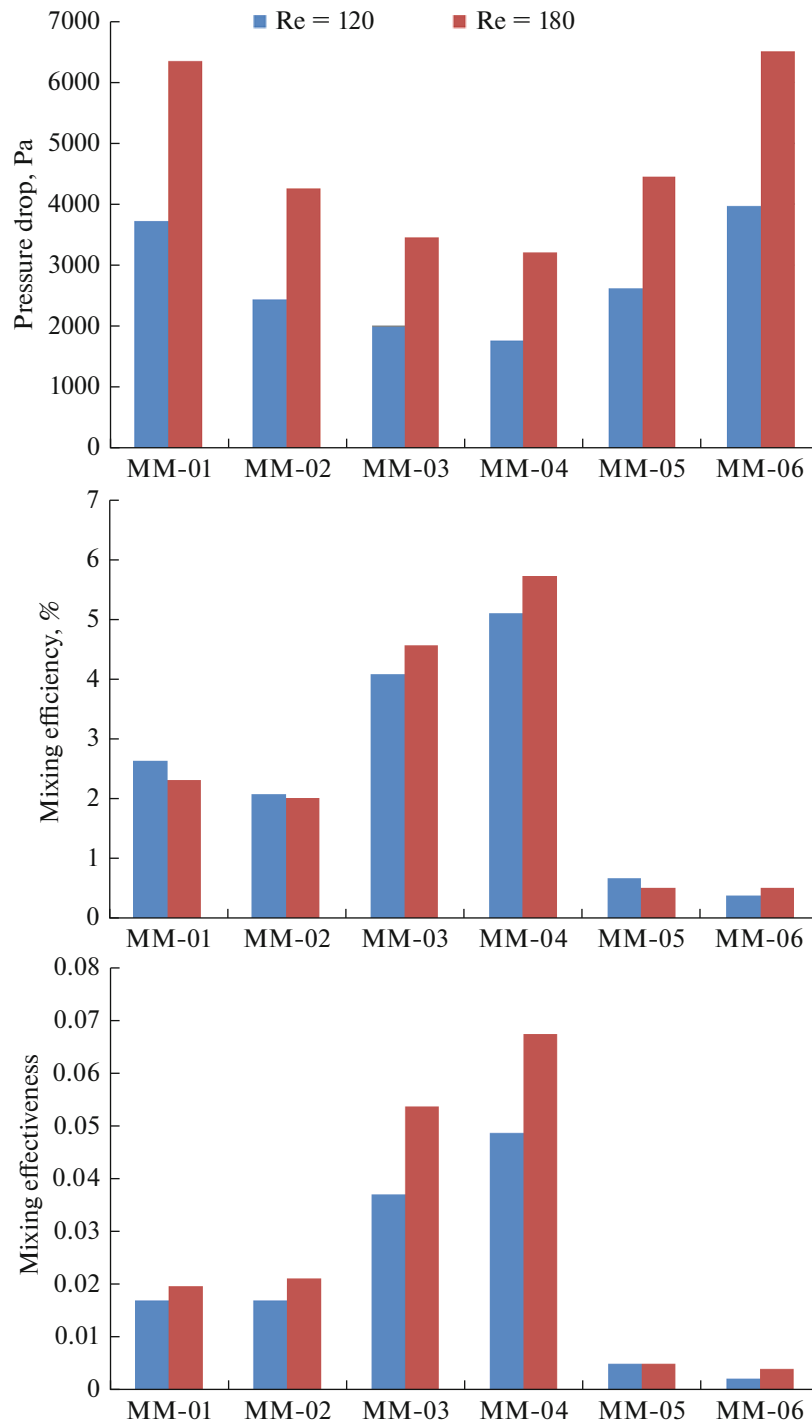


Fig. 6. Pressure drop, mixing efficiency and mixing effectiveness in various micromixers.

angles, the pressure drop is low since the flow path is smooth. When angle is large, the two fluids collide with each other from opposite direction. This increases the form drag and hence the pressure drop. The increase in pressure drop continues up to 120° for MM-03 and 105° for MM-04. At further increased angles e.g. 135° in MM-03, since the flow path again

tends to become relatively smooth, the pressure loss reduces. MM-04 results in low pressure drop when compared to MM-03 for all angles as it has more width. The mixing efficiency is also found to be low in the microchannel devices which have small angles. This is a result of a relatively streamlined flow of the two fluids in the mixing channel. The mixing improves

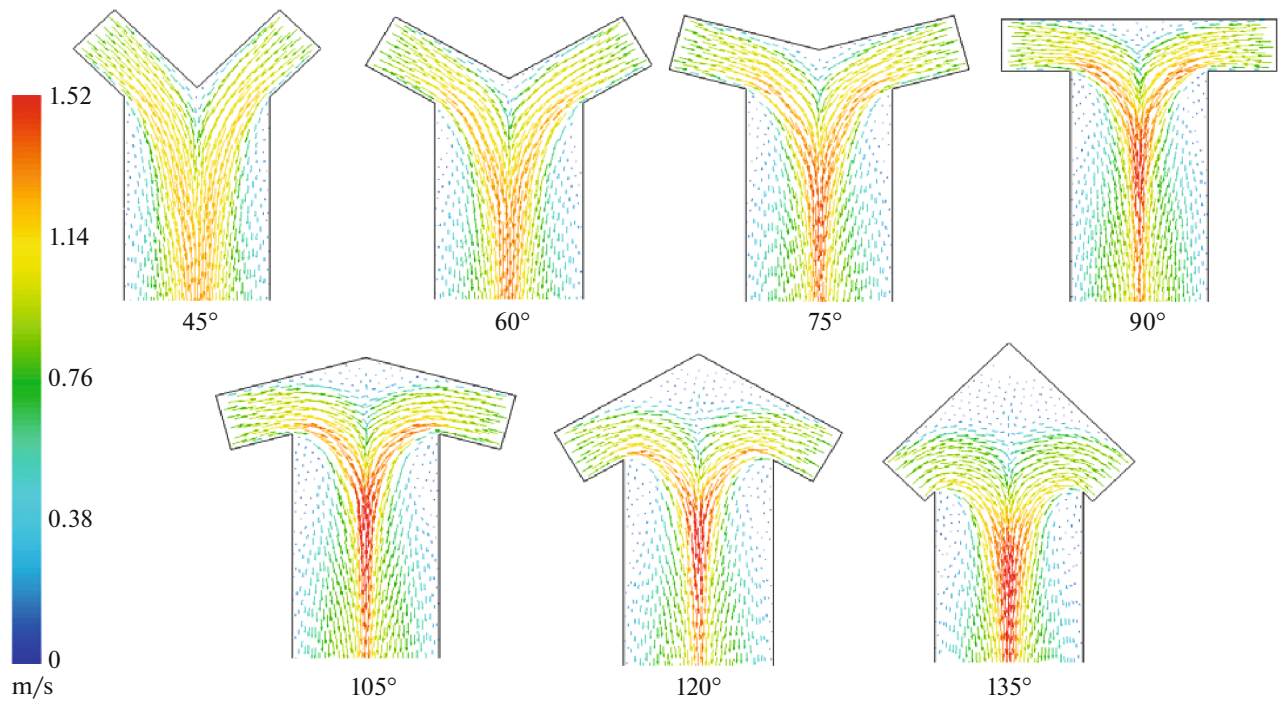


Fig. 7. Effect of confluence angle on velocity profiles (MM-04, Re = 180).

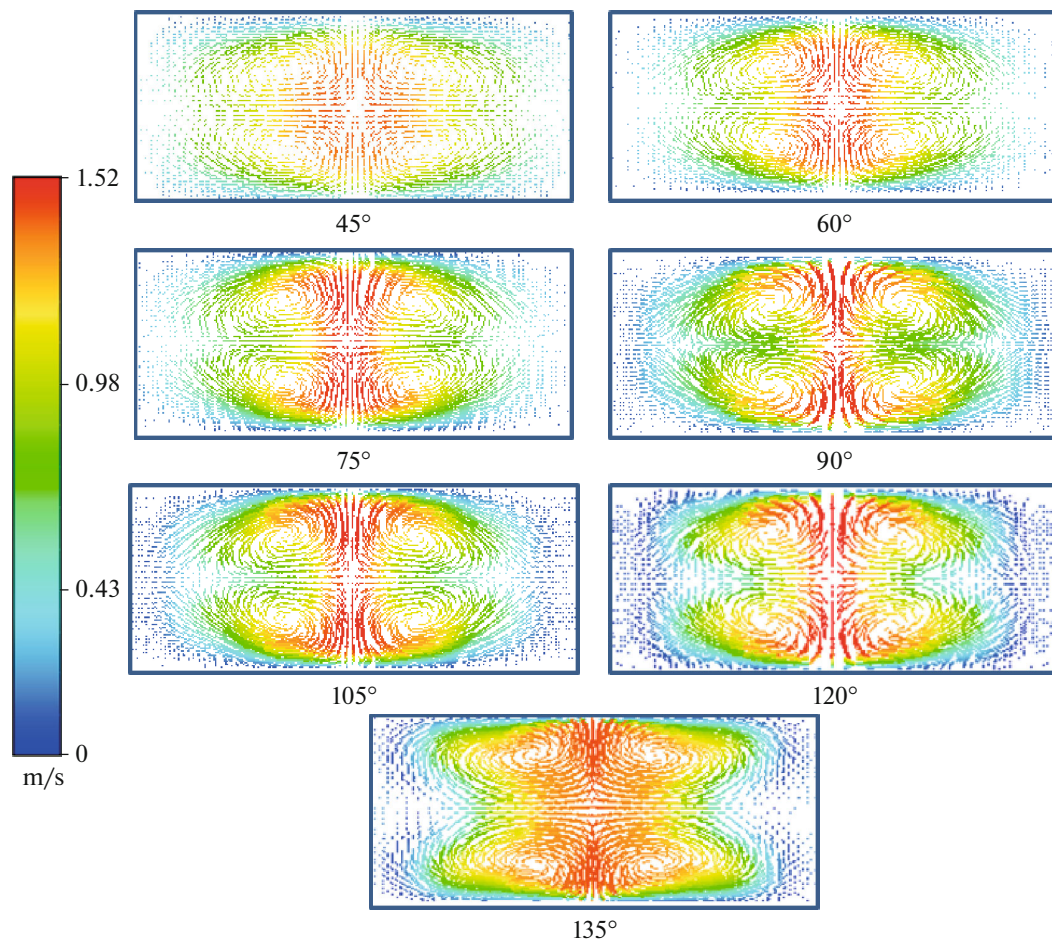


Fig. 8. Velocity vectors at a plane 500 μm measured from inlet section of the mixing channel (MM-04, Re = 180).

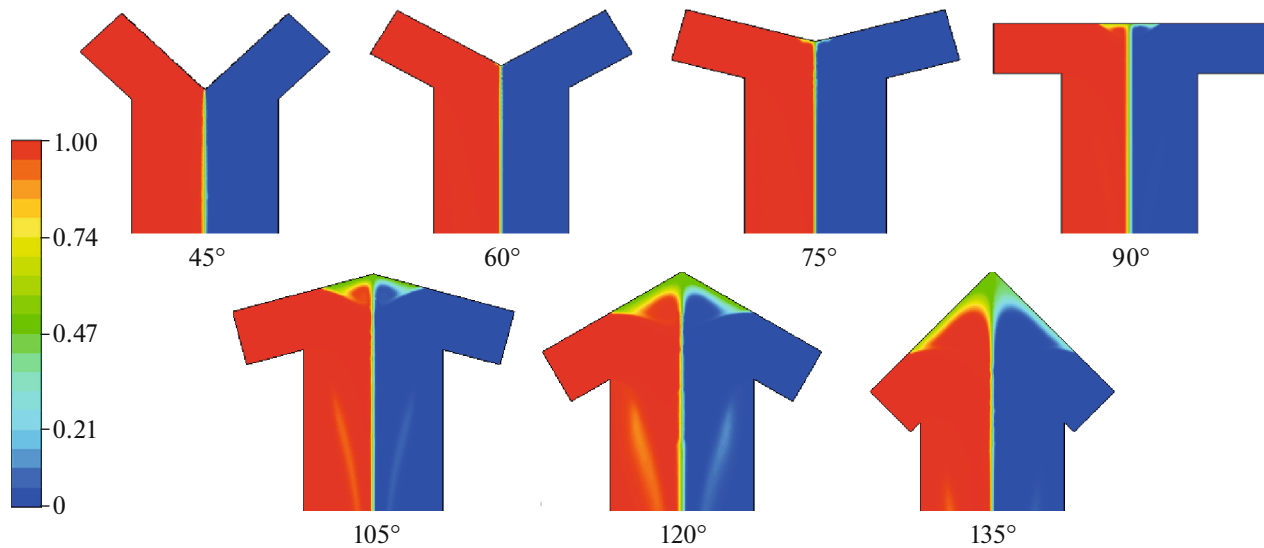


Fig. 9. Contours of tracer mass fraction for different angles of confluence (MM-04, $Re = 180$).

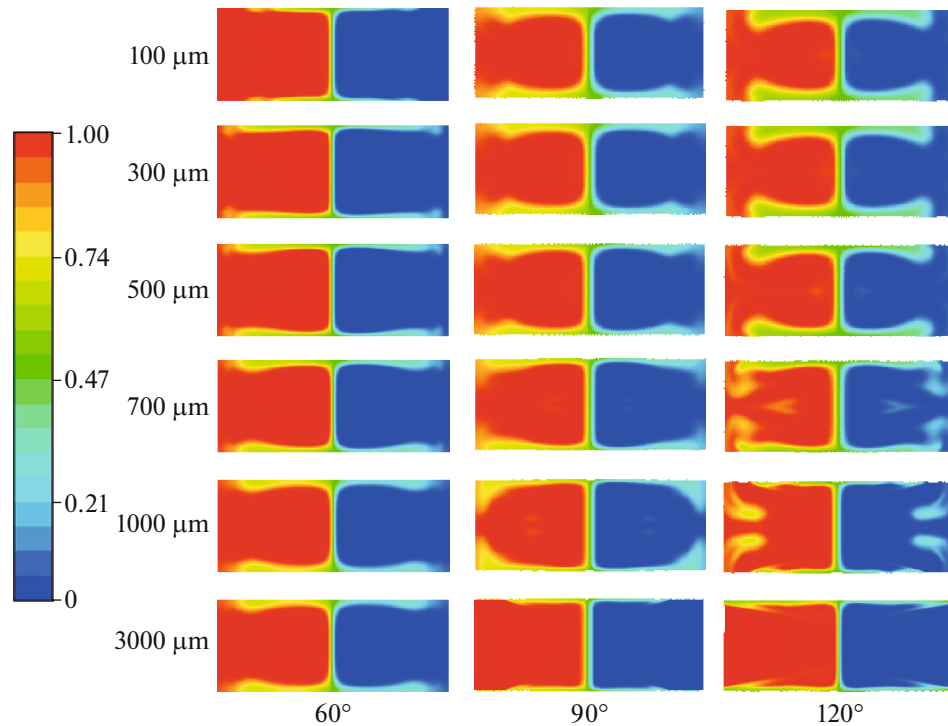


Fig. 10. Variation of mass fraction in 60° , 90° and 120° micromixer geometries versus y -distance ($Re = 180$, MM-04).

at large angles due to fluids collision/contact directly from opposite directions and their rapid turning at the entrance of the mixing channel. The effect of channel aspect ratios can also be observed on the mixing efficiency. At large angles, MM-03 is slightly better than MM-04 in terms of mixing efficiency. The optimal angle for MM-03 and MM-04 both is found to be 120° . At further large value of angle i.e. $\theta = 135^\circ$, the

two fluids although take a sharp turn but they are not perfectly in opposite direction. The interaction is therefore relatively weak which decreases mixing. The mixing effectiveness, similar to the mixing efficiency, has a maximum value when $\theta = 120^\circ$.

The results of CFD modelling in this paper are also compared with the other studies. The friction factors f are calculated for T-shaped MM-01 using equation (8)

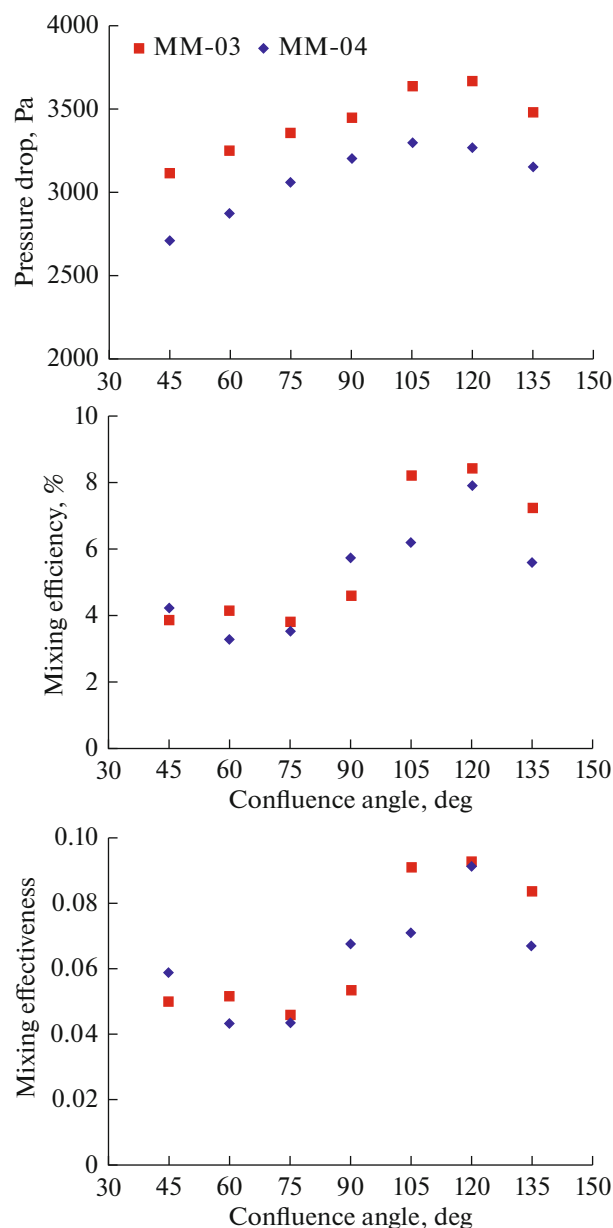


Fig. 11. Pressure drop, mixing efficiency and mixing effectiveness versus confluence angle for MM-03 and MM-04 ($Re = 180$).

and compared with the results obtained by Aoki et al. [8] in an experimental study. The f values in Fig. 12 show reasonable agreement as the difference is within the acceptable range (less than 20%).

CONCLUSIONS

The computational study in this paper analyzes mixing performance of the micromixers with varying channel dimensions. The analysis reveals that the micromixer geometry significantly affects the flow distribution, circulation, pressure losses and the mix-

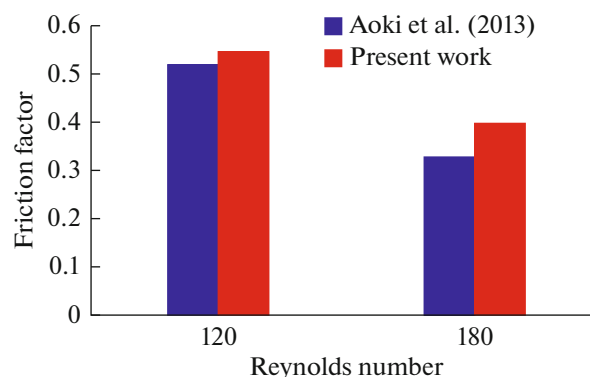


Fig. 12. Comparison of friction factors with experimental work of Aoki et al. [8].

ing characteristics of the device. The geometries with small width to height ratios for outlet channel generally have low mixing efficiency. The increase in width at constant height increases vortex flow motion or circulation which improves mixing rate. An important finding is that the increase in width along with the decrease in height significantly declines micromixer performance even though the cross-sectional area is kept constant. The confluence angle is also varied in the range of 45° – 135° . At small angles, the flow path is organized and well-defined and there is no rapid change in fluid direction while at large angles, the two fluids almost hit from opposite directions and the flow behavior is relatively irregular. The disorganized/irregular fluid structure enhances the mixing process. The overall comparison indicates an optimal confluence angle of 120° for the micromixer device since the mixing efficiency is almost twice when compared to small angles. The CFD results are also compared with the results of previous studies and a satisfactory agreement is found.

ACKNOWLEDGMENTS

The support provided by the NED University of Engineering and Technology is acknowledged.

CONFLICT OF INTEREST

The authors declare that they have no conflicts of interest.

NOTATION

\bar{c}	mean mass fraction of tracer
c	mass fraction of tracer
d_h	hydraulic diameter (m)
D_{AB}	diffusion coefficient (m^2/s)
Eu	Euler number

f	friction factor
h	height of inlet channel
H	height of outlet channel
L_m	length of mixing channel
L_t	length of tracer inlet channel
L_w	length of water inlet channel
ΔP	pressure drop (Pa)
Q_t	total flow rate
Re	Reynolds number
t_m	mixing time (s)
t_r	residence time (s)
u_{av}	average velocity (m/s)
u_y	y-component of velocity (m/s)
w	width of inlet channel
W	width of outlet channel
η	mixing efficiency
ρ	density (kg/m ³)
σ	standard deviation of mass fraction of tracer
μ	viscosity (kg/(m s))
ν	kinematic viscosity (m ² /s)
ω	circulation

REFERENCES

- Hessel, V., Löwe, H., and Schönfeld, F., Micromixers—A review on passive and active mixing principles, *Chem. Eng. Sci.*, 2005, vol. 60, pp. 2479–2501. <https://doi.org/10.1016/j.ces.2004.11.033>
- Jeong, G.S., Chung, S., Kim, C.-B., and Lee, S.-H., Applications of micromixing technology, *Analyst* (Cambridge, U. K.), 2010, vol. 135, no. 3, pp. 460–473. <https://doi.org/10.1039/B921430E>
- Lee, C.Y. and Fu, L.M., Recent advances and applications of micromixer, *Sens. Actuators, B*, 2018, vol. 259, pp. 677–702.
- Capretto, L., Cheng, W., Hill, M., and Zhang, X., Micromixing within microfluidic devices, *Top. Curr. Chem.*, 2011, vol. 304, pp. 27–68.
- Nguyen, N.T. and Wu, Z., Micromixers – A review, *J. Micromech. Microeng.*, 2015, vol. 15, pp. 1–16.
- Bayareh, M., Ashani, M.N., and Usefian, A., Active and passive micromixers: A comprehensive review, *Chem. Eng. Process.*, 2020, vol. 147, article no. 107771. <https://doi.org/10.1016/j.cep.2019.107771>
- Kockmann, N., Kiefer, T., Engler, M., and Woias, P., Convective mixing and chemical reactions in microchannels with high flowrates, *Sens. Actuators, B*, 2006, vol. 117, pp. 495–508.
- Aoki, N., Fukuda, T., Maeda, N., and Mae, K. Design of confluence and bend geometry for rapid mixing in microchannels, *Chem. Eng. J.*, 2013, vol. 227, pp. 198–202.
- Kothare, M.V., Dynamics and control of integrated microchemical systems with application to micro-scale fuel processing, *Comput. Chem. Eng.*, 2006, vol. 30, pp. 1725–1734.
- Yoshimur, M., Shimoyama, K., Misaka, T., and Obayashi, S., Optimization of passive grooved micromixers based on genetic algorithm and graph theory, *Microfluid. Nanofluid.*, 2019, vol. 23, p. 30.
- Taheri, R.A., Goodarzi, V., and Allahverdi, A., Mixing performance of a cost-effective split-and-recombine 3D micromixer fabricated by xurographic method, *Micromachines*, 2019, vol. 10, no. 11, p. 786. <https://doi.org/10.3390/mi10110786>
- Rahimi, M., Azimi, N., Parsamogadam, M.A., Rahimi, A., and Masahy, M.M., Mixing performance of T, Y and oriented Y-micromixers with spatially arranged outlet channel: evaluation with Villermaux/Dushman test reaction, *Microsyst. Technol.*, 2017, vol. 23, pp. 3117–3130.
- Hsieh, S.S., Lin, J.W., and Chen, J.W., Mixing efficiency of Y-type micromixers with different angles, *Int. J. Heat Fluid Flow*, 2013, vol. 44, pp. 130–139.
- Lobasov, A.S., Minakov, A.V., Kuznetsov, V.V., Rudyak, V.Y., and Shebeleva, A.A., Investigation of mixing efficiency and pressure drop in T-shaped micromixers, *Chem. Eng. Process.*, 2018, vol. 134, pp. 105–114.
- Wong, S.H., Ward, M., Wharton, C.W., and Shenoy, K.T., Micro T-mixer as a rapid mixing micromixer, *Sens. Actuators, B*, 2004, vol. 100, pp. 359–379.
- Silva, J.P., Santos, A., and Semiao, V., Experimental characterization of pulsed Newtonian fluid flows inside T-shaped micromixers with variable inlets widths, *Exp. Therm. Fluid Sci.*, 2017, vol. 89, pp. 249–258.
- Ansari, M.A., Kim, K.Y., Anwar, K., and Kim, S.M., Vortex micro T-mixer with non-aligned inputs, *Chem. Eng. J.*, 2012, vols. 181–182, pp. 846–850.
- Calado, B., Santos, A., and Semiao, V., Characterization of the mixing regimes of Newtonian fluid flows in asymmetrical T-shaped micromixers, *Exp. Therm. Fluid Sci.*, 2016, vol. 72, pp. 218–222.
- You, J.B., Choi, Y., and Im, S.G., Influence of adjusting the inlet channel confluence angle on mixing behavior, *Microfluid. Nanofluid.*, 2017, vol. 21, pp. 121–128.
- Chen, Y., Chen, X., and Liu, S., Numerical and experimental investigations of novel passive micromixers with fractal-like tree structures, *Chem. Phys. Lett.*, 2020, vol. 747, article no. 137330.
- Soleymani, A., Yousefi, H., and Turunen, I., Dimensionless number for identification of flow patterns inside a T-micromixer, *Chem. Eng. Sci.*, 2008, vol. 63, pp. 5291–5297.
- Cortes-Quiroz, C.A., Azarbadegan, A., and Zangeneh, M., Evaluation of flow characteristics that give higher mixing performance in the 3-D T-mixer versus the typical T-mixer, *Sens. Actuators, B*, 2014, vol. 202, pp. 1209–1219.
- Fatima, U., Shakaib, M., and Memon, I., Analysis of mass transfer performance of micromixer device with varying confluence angle using CFD, *Chem. Pap.*, 2020, vol. 74, pp. 1267–1279.
- Naher, S., Orpen, D., Brabazon, D., Poulsen, C.R., and Morshed, M.M., Effect of micro-channel geometry on fluid flow and mixing, *Simul. Modell. Pract. The-*

- ory, 2011, vol. 19, no. 4, pp. 1088–1095.
<https://doi.org/10.1016/j.simpat.2010.12.008>
25. Alam, A., Afzal, A., and Kim, K.Y., Mixing performance of a planar micromixer with circular obstructions in a curved microchannel, *Chem. Eng. Res. Des.*, 2014, vol. 92, pp. 423–434.
 26. Wang, L., Liu, D., Wang, X., and Han, X., Mixing enhancement of novel passive microfluidic mixers with cylindrical grooves, *Chem. Eng. Sci.*, 2012, vol. 81, pp. 157–163.
 27. Kashid, M., Renken, A., and Kiwi-Minsker, L., Mixing efficiency and energy consumption for five generic microchannel designs, *Chem. Eng. J.*, 2011, vol. 167, pp. 436–443.
 28. Jeon, W. and Shin, C.B., Design and simulation of passive mixing in microfluidic systems with geometric variations, *Chem. Eng. J.*, 2009, vol. 152, pp. 575–582.
 29. Aubin, J., Fletcher, D.F., and Xuereb, C., Design of micromixers using CFD modelling, *Chem. Eng. Sci.*, 2005, vol. 60, nos. 8–9, pp. 2503–2516.
<https://doi.org/10.1016/j.ces.2004.11.043>
 30. Kakavandi, F., Rahimi, M., Jafari, O., and Azimi, N., Liquid-liquid two phase mass transfer in T-type micromixers with different junctions and cylindrical pits, *Chem. Eng. Process.*, 2018, vol. 85, pp. 58–67.
 31. Amar, K., Embarek, D., and Sofiane, K., Parametric study of the Crossing elongation effect on the mixing performances using short Two-Layer Crossing Channels Micromixer (TLCCM) geometry, *Chem. Eng. Res. Des.*, 2020, vol. 158, pp. 33–43.
 32. Hossain, S., Ansari, M.A., and Kim, K., Evaluation of the mixing performance of three passive micromixers, *Chem. Eng. J.*, 2009, vol. 150, pp. 492–501.
 33. Chung, C.K. and Shih, T.R., Effect of geometry on fluid mixing of the rhombic micromixers, *Microfluid. Nanofluid.*, 2008, vol. 4, pp. 419–425.
 34. Fang, Y., Ye, Y., Shen, R., Zhu, P., Guo, R., Hu, Y., and Wu, L., Mixing enhancement by simple periodic geometric features in microchannels, *Chem. Eng. J.*, 2012, vol. 187, pp. 306–310.
 35. Borgogna, A., Murmura, M.A., Annesini, M.C., Gianna, M., and Cerbelli, S., A hybrid numerical approach for predicting mixing length and mixing time in microfluidic junctions from moderate to arbitrarily large values of the Péclet number, *Chem. Eng. Sci.*, 2019, vol. 196, pp. 247–264.
 36. Borgogna, A., Murmura, M.A., Annesini, M.C., Gianna, M., and Cerbelli, S., Inertia-driven enhancement of mixing efficiency in microfluidic cross-junctions: A combined Eulerian/Lagrangian approach, *Microfluid. Nanofluid.*, 2018, vol. 22, p. 20.
<https://doi.org/10.1007/s10404-018-2041-9>
 37. Engler, M., Kockmann, N., Kiefer, T., and Woias, P., Numerical and experimental investigations on liquid mixing in static micromixers, *Chem. Eng. J.*, 2004, vol. 101, pp. 315–322.